Acta Crystallographica Section B
Structural Science
ISSN 0108-7681

Monitoring structural transformations in crystals. 12. Course of an intramolecular [4 + 4] photocycloaddition in a crystal

Elżbieta Trzop and Ilona Turowska-Tyrk*

Faculty of Chemistry, Wrocław University of Technology, Wybrzeże Wyspiańskiego 27, 50-370 Wrocław, Poland

Correspondence e-mail: ilona.turowska-tyrk@pwr.wroc.pl

Received 7 February 2008
Accepted 10 April 2008

For Part 11 see Turowska-Tyrk, Bąkowicz & Scheffer (2007).

Variations in crystal and molecular structures, brought about by the intramolecular [4 + 4] photocycloaddition of bi(anthracene-9,10-dimethylene), were monitored using X-ray diffraction. The cell volume increased by 0.8% until the reaction was *ca* 40% complete, and afterwards decreased by 1.6% during the remainder of the photoreaction. The changes of the *a* and *b* lattice parameters were correlated with the changes of the molecular shape and packing. The distance between the directly reacting C atoms varied in a manner not observed for other photochemical reactions in crystals. It was constant until *ca* 20% photoreaction progress, then decreased, and later stabilized from *ca* 40% photoreaction progress. This phenomenon was explained by interplay between stress resulting from the presence of product molecules and the rigidity of reactant molecules. Changes of the orientation of molecules during the photoreaction were smaller than in the case of other monitored photochemical reactions in crystals owing to similarities in the shape and packing of reactant and product molecules. Weak C—H$\cdots\pi$ hydrogen bonds exist among reactant molecules in the pure reactant and partly reacted crystals.

1. Introduction

Although photochemical reactions in crystals are often discussed in the scientific literature, single-crystal-to-single-crystal photochemical reactions are rather rare. The great advantage of the latter is the possibility of monitoring structural changes brought about by the photoreactions. Such studies demand the determination of structures for many steps on the way leading from a pure reactant crystal to a pure product crystal. The structures determined for each of the steps are slightly different. Detailed analysis of them enables one to monitor molecules in a crystal and a reaction centre in molecules. In some cases it can help to explain the formation of additional products in crystals (Turowska-Tyrk, Bąkowicz, Scheffer & Xia, 2006; Turowska-Tyrk, Łabęcka, Scheffer & Xia, 2007).

The aim of our studies carried out in recent years was the monitoring of structural changes in crystals by means of X-ray structure analysis. We concentrated on intermolecular [2 + 2] and [4 + 4] photocycloadditions (Turowska-Tyrk, 2001, 2003; Turowska-Tyrk & Trzop, 2003) and the unimolecular formation of a cyclobutane ring, namely the Yang photocycloaddition (Turowska-Tyrk, Bąkowicz & Scheffer, 2007; Turowska-Tyrk, Łabęcka, Scheffer & Xia, 2007; Turowska-Tyrk, Trzop, Scheffer & Chen, 2006). It should be emphasized that [2 + 2] photocycloadditions were also monitored by others (Fernandes & Levendis, 2004; Ohba & Ito, 2003).

In this paper we present an analysis of structural changes proceeding in crystals during the intramolecular [4 + 4] photocycloaddition of bi(anthracene-9,10-dimethylene) (1). The equation of the photoreaction is presented in (I). In this photoreaction two new single bonds are formed between the middle rings of the anthracene systems, which causes a loss of aromatic character of both rings. Sensitivity of (1) to visible light and formation of photoproduct (2) were discovered by Golden (1961). The photoreaction can take place in a solution and the solid state, and may proceed even at 4 K (Fergusson & Mau, 1974; Fergusson *et al.*, 1973; Wada & Tanaka, 1977). Reversal of the photoreaction in the dark with time and temperature was also reported (Dougherty *et al.*, 1986; Golden, 1961; Kaupp, 1972*a*,*b*).

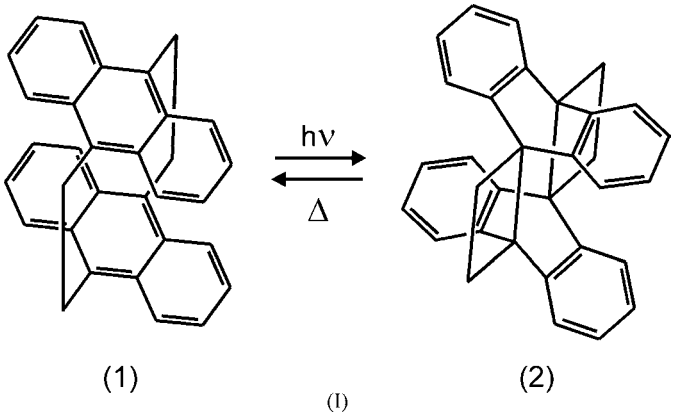

(I)

The [4 + 4] photocycloaddition of (1) proceeds in a single-crystal-to-single-crystal manner (Dougherty *et al.*, 1986; Harada *et al.*, 1995, 1996; Kaupp, 1995, 2002). Structures of (1) (Harada *et al.*, 1995, 1996; Milledge, 1962; Wada & Tanaka, 1977) and (2) (Battersby *et al.*, 1995; Dougherty *et al.*, 1986; Ehrenberg, 1966; Harada *et al.*, 1995, 1996) were already published. The structure determined from the pure photoproduct by Ehrenberg (1966) was in fact a combination of the photoproduct and a small amount of the reactant (Harada *et al.*, 1995, 1996). Nevertheless, the reported reactant–product disorder was not solved. Moreover, no structures were published for intermediate steps on the way from a pure reactant crystal to a pure photoproduct crystal and the course of this photoreaction is unknown.

2. Experimental

Crystals of (1) were recrystallized from chloroform:toluene (1:1). All experiments were conducted in the dark because of the high sensitivity of (1) to daylight. The experiments were carried out for five single crystals, four of them were already partly reacted. All crystals were irradiated in steps using an Hg 100 W lamp, a GG-420 glass filter (0% transmittance for $\lambda <$ 410 nm and *ca* 95% transmittance for $\lambda >$ 460 nm) or GG-455 (0% transmittance for $\lambda <$ 440 nm and *ca* 95% transmittance for $\lambda >$ 485 nm) and a water filter. The glass filters were chosen on the basis of an absorption spectrum of (1) (Masnovi *et al.* 1985). The transmitted wavelengths of the low-energy tail ensured good crystal penetration and homogeneity of the photoreaction (Enkelman *et al.* 1993; Novak *et al.*, 1993*a*,*b*). The beam was perpendicular to the longest crystal edges. The crystals were rotated during irradiation. The irradiation times were: crystal (1): 0, 2, 6, 10 and 15 min; crystal (2): 1 min; crystal (3): 5 and 10 min; crystal (4): 5 min; crystal (5): 30 min. All were irradiated at ambient temperature. Crystal (5) was examined once again 14 days after the day of the irradiation.

Immediately after each irradiation of the crystal, X-ray data were collected by means of a CCD diffractometer (Oxford Diffraction, 2003). The general strategy for data collection using area-detector diffractometers was described by Scheidt & Turowska-Tyrk (1994). The cell constants were determined on the basis of the 1000 strongest reflections. The percentage of well indexed reflections for the pure reactant and pure product crystals was 99.9 and 98.3%, respectively. In the case of the partly reacted crystals, this was in the range 96.7–100%. This fit indicates that the photoreaction took place homogenously, *i.e.* at no time was there any macroscopic domain formation of the reactant or the product. Moreover, neither a significant increase in the size of the reflections nor any reflection splitting was observed as the photoreaction progressed. The intensities of the reflections were corrected for Lorentz and polarization effects (Oxford Diffraction, 2003).

The structure determination was completed for 0, 4.3 (4), 9.9 (6), 14.6 (8) and 16.2 (8)% product content [crystal (1)], 18.3 (9)% product content [crystal (2)], 32.4 (10) and 38.6 (12)% [crystal (3)], 84.6 (10)% [crystal (4)], 63.9 (14) and 100% [crystal (5)]. The percentage of the product was determined during structure refinements from the site-occupation factors. Initial atomic coordinates for the pure reactant and pure product crystals were taken from Harada *et al.* (1995, refcodes ANTMEU01 and ANTMET03); all non-H atoms were refined anisotropically. For the partly reacted crystals, initial atomic coordinates of the major component were taken from the pure reactant or pure product structures determined by us. The first non-H atoms of the minor component were found in difference-Fourier maps and the remaining atoms were located geometrically. In most cases the major component was refined anisotropically and the minor component isotropically. Only for the crystals of 63.9 (14) and 84.6 (10)% product content were the C9–C14 atoms of the major component refined isotropically. For all crystals the positions of the H atoms were found geometrically and refined with constraints.

During the structure determination of the partly reacted crystals, the use of constraints and restraints for geometrical and displacement parameters was necessary. The following instructions from *SHELXL*97 (Sheldrick, 2008) were applied: AFIX, DFIX, DANG, FLAT and SIMU. The AFIX constraint was used to generate the idealized coordinates and displacement parameters of the H atoms. The DFIX and DANG commands were applied to weakly restrain bond lengths and valence angles to target values. The target values were taken from the structures of the pure reactant and the pure photoproduct. The FLAT command restrained some atoms to be coplanar. SIMU restrained the displacement parameters of

Table 1
Experimental details.

	9.9%P	18.3%P	32.4%P	84.6%P
Crystal data				
Crystal number	(1)	(2)	(3)	(4)
Chemical formula	$C_{32}H_{24}$	$C_{32}H_{24}$	$C_{32}H_{24}$	$C_{32}H_{24}$
M_r	408.51	408.51	408.51	408.51
Cell setting, space group	Monoclinic, $P2_1/c$	Monoclinic, $P2_1/c$	Monoclinic, $P2_1/c$	Monoclinic, $P2_1/c$
Temperature (K)	299 (2)	299 (2)	299 (2)	299 (2)
a, b, c (Å)	10.285 (2), 12.791 (2), 8.4484 (18)	10.2742 (15), 12.8086 (15), 8.4500 (12)	10.264 (2), 12.8929 (19), 8.4043 (17)	9.961 (5), 12.976 (4), 8.504 (2)
β (°)	113.05 (3)	112.999 (17)	112.34 (2)	111.86 (4)
V (Å^3)	1022.7 (3)	1023.6 (2)	1028.7 (3)	1020.1 (6)
Z	2	2	2	2
D_x (Mg m^{-3})	1.327	1.325	1.319	1.330
Radiation type	Mo $K\alpha$	Mo $K\alpha$	Mo $K\alpha$	Mo $K\alpha$
μ (mm^{-1})	0.08	0.08	0.07	0.08
Crystal form, colour	Plate, orange	Plate, orange	Plate, orange	Plate, pale yellow
Crystal size (mm)	0.55 × 0.33 × 0.15	0.45 × 0.30 × 0.12	0.34 × 0.28 × 0.12	0.32 × 0.22 × 0.10
Data collection				
Diffractometer	Kuma KM4CCD	Kuma KM4CCD	Kuma KM4CCD	Kuma KM4CCD
Data collection method	ω scans	ω scans	ω scans	ω scans
Absorption correction	None	None	None	None
No. of measured, independent and observed reflections	5204, 1786, 1291	5405, 1776, 1032	5354, 1788, 1055	5328, 1794, 835
Criterion for observed reflections	$I > 2\sigma(I)$	$I > 2\sigma(I)$	$I > 2\sigma(I)$	$I > 2\sigma(I)$
R_{int}	0.018	0.034	0.051	0.105
θ_{max} (°)	25.0	25.0	25.0	25.0
Refinement				
Refinement on	F^2	F^2	F^2	F^2
$R[F^2 > 2\sigma(F^2)]$, $wR(F^2)$, S	0.048, 0.148, 1.07	0.060, 0.195, 1.06	0.076, 0.243, 1.08	0.121, 0.368, 1.16
No. of reflections	1786	1776	1788	1794
No. of parameters	211	211	211	180
H-atom treatment	Constrained to parent site	Constrained to parent site	Constrained to parent site	Constrained to parent site
Weighting scheme	$w = 1/[\sigma^2(F_o^2) + (0.0761P)^2 + 0.2388P]$, where $P = (F_o^2 + 2F_c^2)/3$	$w = 1/[\sigma^2(F_o^2) + 0.0901P)^2 + 0.3636P]$, where $P = (F_o^2 + 2F_c^2)/3$	$w = 1/[\sigma^2(F_o^2) + (0.1311P)^2 + 0.2212P]$, where $P = (F_o^2 + 2F_c^2)/3$	$w = 1/[\sigma^2(F_o^2) + (0.2P)^2]$, where $P = (F_o^2 + 2F_c^2)/3$
$(\Delta/\sigma)_{max}$	< 0.0001	< 0.0001	0.001	< 0.0001
$\Delta\rho_{max}$, $\Delta\rho_{min}$ (e Å^{-3})	0.18, −0.16	0.18, −0.15	0.26, −0.24	0.34, −0.39

Computer programs used: *CRYSALIS* (Oxford Diffraction Ltd, 2003), *SHELXL*97 (Sheldrick, 2008), *ORTEP*3 for Windows (Farrugia, 1997).

several atoms of the reactant and the photoproduct. For all partly reacted crystals, the same, or almost the same, constraints and restraints were applied. There were small differences between refinements in the number of SIMU and FLAT restraints. The C9—C10^{i} bond length in the photoproduct molecule was restrained to the value observed in the crystal of the pure photoproduct. Neither restraints nor constraints were used for the C9···C10^{i} distance in the reactant molecule.

Selected experimental data are given in Table 1 for four of the structures. Data for all structures are given in the supplementary material.[2] In order to check the stability of the photoproduct in the absence of visible radiation, an additional data collection was carried out 12 h after the data collection for one of the partly reacted crystals. The content of the product determined was statistically the same for both cases. This structure determination also showed that the photoreaction was not influenced by X-rays. Additionally, it was checked that the crystal of the pure photoproduct (2) needs more than 1 month at ambient temperature to return to the crystal of the pure reactant (1) (14 d to return to the crystal containing 63.9% of the photoproduct).

[2] Supplementary data for this paper are available from the IUCr electronic archives (Reference: BK5072). Services for accessing these data are described at the back of the journal.

3. Results and discussion

3.1. Monitoring the cell constants and the cell volume

Changes of the crystal structure are reflected in, among other things, changes of the cell constants. Fig. 1 presents the dependence between the values of the cell constants and the percentage content of the product in the crystal for the photoreaction of (1). As can be seen, the *a* parameter is constant until *ca* 40% crystal conversion, and afterwards decreases smoothly by 0.420 (2) Å until the end of the photoreaction. The reason for this decrease will be discussed

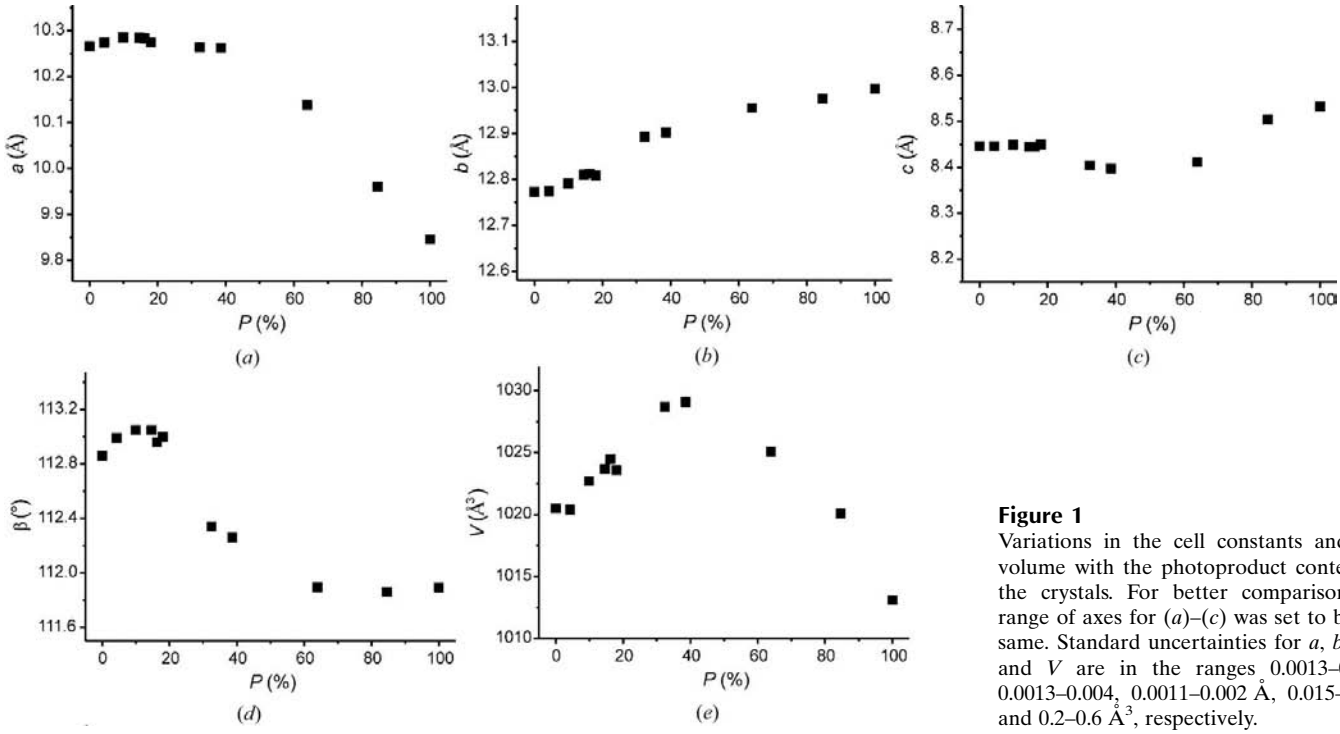

Figure 1
Variations in the cell constants and cell volume with the photoproduct content in the crystals. For better comparison the range of axes for (*a*)–(*c*) was set to be the same. Standard uncertainties for *a*, *b*, *c*, β and *V* are in the ranges 0.0013–0.005, 0.0013–0.004, 0.0011–0.002 Å, 0.015–0.04° and 0.2–0.6 Å^3, respectively.

in the next paragraph. In turn the *b* parameter increases by 0.224 (2) Å, however, at the beginning of the photoreaction this increase is small. The *c* cell constant changes in a manner different from *a* and *b*. It is constant during the first 20% of the crystal conversion, afterwards decreases slightly and next increases until the end of the photoreaction. The difference between the values of *c* for the pure reactant and pure product crystals is smaller than in the case of *a* and *b*: 0.0860 (19) Å. The total change of the β angle is very small, 0.97 (2)°, but even here the curve presenting the variations in β is smooth.

The values of *a*, *b*, *c* and β are reflected in the cell volume. The cell volume increases from 1020.5 (3) to 1029.1 (5) Å^3 at *ca* 40% photoreaction progress, *i.e.* by 0.8%, and decreases during the remaining part of the photoreaction to 1013.1 (2) Å^3, *i.e.* it decreases by 1.6% of the cell volume for the pure reactant crystal. The type of variation in the cell volume for the photoreaction of (1) is similar to that for the intermolecular [4 + 4] photocycloaddition of 9-methylanthracene (Turowska-Tyrk & Trzop, 2003). However, in the case of the intermolecular [2 + 2] photocycloadditions (Nakanishi *et al.*, 1980, 1981; Turowska-Tyrk, 2003) and also the intramolecular formation of a cyclobutane ring in the Yang photocycloadditions (Turowska-Tyrk, Bąkowicz & Scheffer, 2007; Turowska-Tyrk, Łabęcka, Scheffer & Xia, 2007; Turowska-Tyrk, Trzop, Scheffer & Chen, 2006), no similarities between types of variations in the cell volume were observed. Moreover, the size of the change was also different for different compounds undergoing the same kind of photochemical reaction. The relevant data are presented in Table 2.

3.2. Molecular shape and crystal packing

The variations in the lattice parameters reflect variations in the molecular and crystal structures. Since a picture of a molecule obtained from X-ray structure analysis is averaged over a crystal volume, for the partly reacted crystals we can see reactant molecule (1) superimposed on product molecule (2). Fig. 2 presents an example of such a disorder. As can be seen, all atoms of the structure were separated between the reactant and the product. Such separation was possible for all partly reacted crystals. The reactant and product molecules are situated on an inversion centre and only their halves are symmetrically independent.

The overall shapes of the product and reactant molecules are quite similar. However, certain differences can also be noticed, for instance, the butterfly-like shape of product molecules. This fact should have an impact on crystal packing. Projections of the crystal lattice of reactant (1) and photoproduct (2) on the *ab* plane are presented in Fig. 3. As can be seen, the packing in the two crystals differs slightly in the central part of the unit cell. The void space in this region is smaller in the pure photoproduct crystal than the pure reactant crystal. In order to describe this observation quantitatively, we defined parameters l_1 and l_2 as the distances between the centres of the external rings of the closest neighbouring molecules. The angles between the *a* axis and the directions of l_1 and l_2 are 12.5 and 24.2°, respectively. The values of l_1 and l_2 decrease with the photoreaction progress: l_1 is 5.74 and 5.53 Å in the pure reactant and pure product crystals, respectively, and l_2 is 5.85 and 5.05 Å, respectively. These decreases may be

Table 2
Changes of the cell constants and the cell volume divided by the number of molecules in the unit cell (Å, Å^3).

Compound	$\Delta a/Z$	$\Delta b/Z$	$\Delta c/Z$	$\Delta V/Z$
5-Benzylidene-2-benzylcyclopentanone[a]†	0.0024 (15)	0.0034 (6)	−0.0072 (5)	−1.3 (3)
5-Benzylidene-2-(4-chlorobenzyl)-cyclopentanone[b]†	−0.1218 (12)	0.0330 (8)	−0.0168 (12)	−10.2 (3)
1-(4-Carboxybenzoyl)-1-methyladamantane salt[c]‡	0.1710 (8)	−0.2498 (10)	−0.0300 (10)	2.2 (4)
2-(4-Carboxybenzoyl)-2-methyl-*endo*-bicyclo[2.1.1]hexyl salt[d]‡	0.0236 (4)	−0.0042 (5)	−0.299 (4)	−7.0 (3)
6,6-Diethyl-5-oxo-5,6,7,8-tetrahydronaphthalene-2-carboxylate salt[e]‡	0.0346 (5)	0.0538 (8)	−0.2630 (18)	−0.8 (2)
(1)[f]	−0.2100 (10)	0.1120 (10)	0.0430 (10)	−3.7 (2)

References: (*a*) Turowska-Tyrk (2001), Nakanishi *et al.* (1981); (*b*) Turowska-Tyrk (2003), Theocharis *et al.* (1981), Jones & Theocharis (1984); (*c*) Turowska-Tyrk, Trzop, Scheffer & Chen (2006), Leibovitch *et al.* (1997); (*d*) Turowska-Tyrk, Łabęcka, Scheffer & Xia (2007); (*e*) Turowska-Tyrk, Bąkowicz & Scheffer (2007); (*f*) this paper. † [2+2] photocycloaddition. ‡ Yang photocyclization.

correlated with the decrease of the *a* lattice parameter. Small differences in the molecular shape, and packing, can also be noticed along the *b* axis.

3.3. Monitoring variations in the geometry of the reaction centre

The [4 + 4] photocycloaddition of (1) proceeds in a topotactic manner (Kaupp, 1995), which means that only small movements of atoms and molecules take place during the photoreaction in crystals. Nevertheless, even such small movements can be monitored and interpreted.

It results from our previous studies of intramolecular photochemical reactions that the geometry of molecules is not constant in crystals, but changes slightly as the photoreaction progresses (Turowska-Tyrk, Bąkowicz & Scheffer, 2007; Turowska-Tyrk, Bąkowicz, Scheffer & Xia, 2006; Turowska-Tyrk, Łabęcka, Scheffer & Xia, 2007; Turowska-Tyrk, Trzop, Scheffer & Chen, 2006). The reason for this fact is that reactant molecules are under the stress of an increasing number of photoproduct molecules which force the reactant to adopt photoproduct-like geometry. In some cases such changes can be of chemical importance. For instance, a decrease in the distance between certain atoms in reactant molecules was a reason for the formation of an additional enantiomorph in the retro-Claisen photorearrangement (Turowska-Tyrk, Bąkowicz, Scheffer & Xia, 2006).

In the case of the photoreaction of (1) we monitored the distance between the atoms which take part directly in the formation of the new bond, *i.e.* C9···C10^{i} [(i) $-x, 1-y, 1-z$; C9^{i}···C10 is symmetrically equivalent]. The results are shown in Fig. 4(*a*). The distance is 2.765 (2) Å in the pure reactant crystal. It is statistically constant during the initial stages of the photoreaction. This can be explained by the fact that at these stages there is only a small number of photoproduct molecules in the crystal and a stress caused by them upon reactant molecules is small. After *ca* 20% crystal conversion this distance decreases by 0.098 (14) Å to 2.667 (12) Å. The observed change is statistically significant at the 3σ level, *i.e.* with 99.7% probability. This decrease is a result of an increasing number of photoproduct molecules and hence an increasing stress caused by them upon reactant molecules. At *ca* 40% conversion C9···C10^{i} becomes statistically constant until the end of the photoreaction. This stability may be the result of the rigidity of reactant molecules owing to the ethylene bridges between the anthracene systems. The ethylene bridges prevent the anthracene systems from coming closer than *ca* 2.65 Å. Variations of this kind were not observed for other intra- and intermolecular photochemical

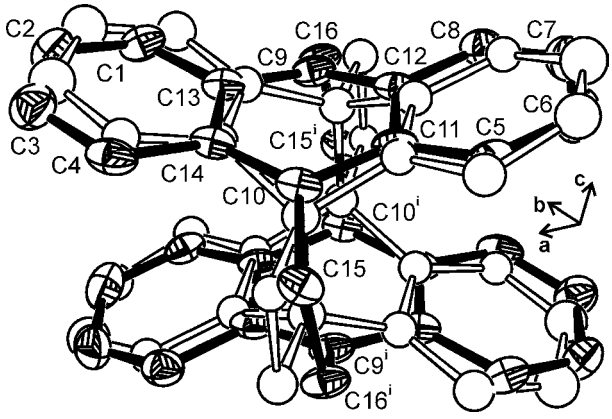

Figure 2
ORTEP (Farrugia, 1997) view of the photoproduct molecule (empty bonds) superimposed on the reactant molecule (filled bonds) for the partly reacted crystal containing 32.4 (10)% of the photoproduct. H atoms are omitted and only reactant atoms are labelled for clarity. Displacement ellipsoids are drawn at the 20% probability level.

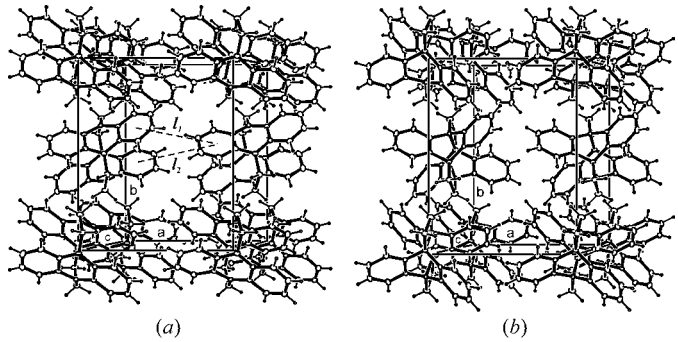

Figure 3
Projection of the crystal lattice of reactant (1) and photoproduct (2) on the *ab* plane.

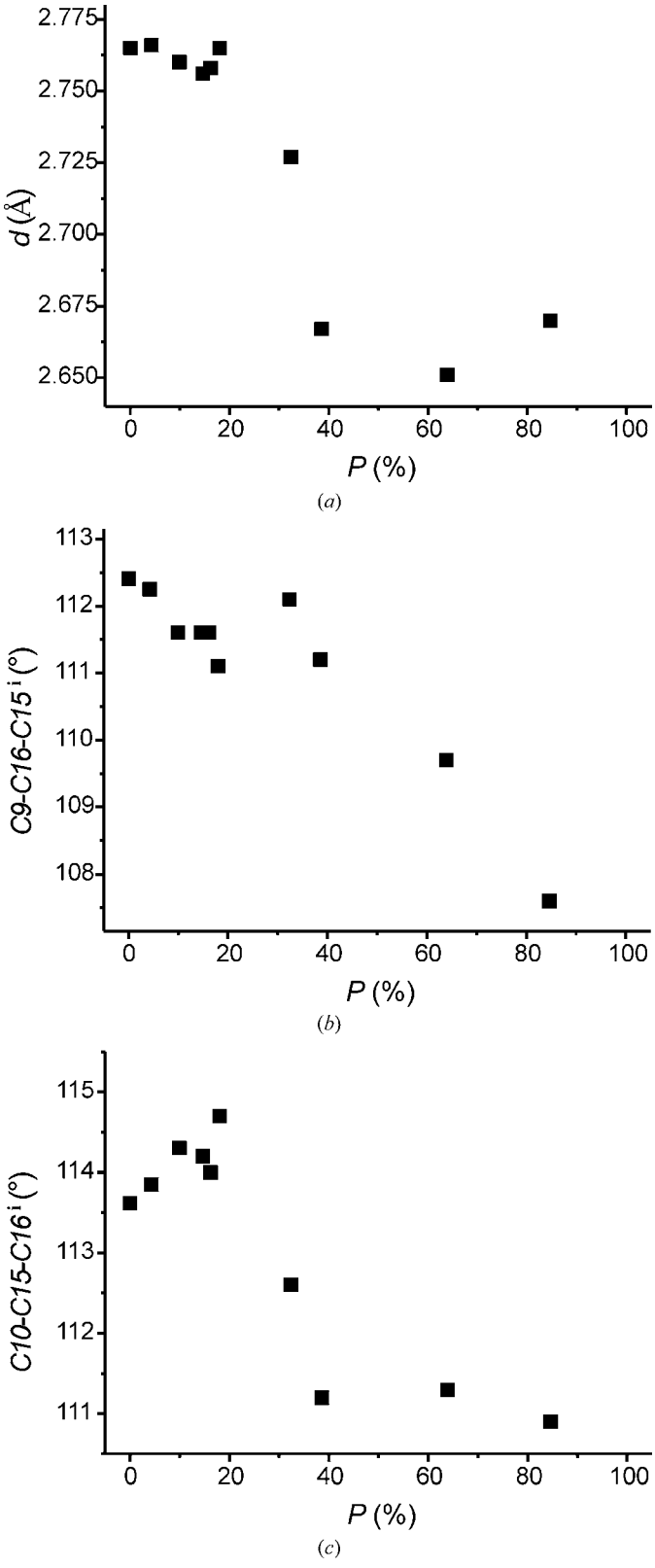

Figure 4
Variations in (*a*) the C9···C10^{i} distance between directly reacting atoms [(i) $-x, 1-y, 1-z$], (*b*) the C9—C16—C15^{i} and (*c*) the C10—C15—C16^{i} valence angles with the photoproduct content in the crystals. Standard uncertainties for the distance and for the valence angles are in the ranges 0.002–0.03 Å, 0.13–0.8 and 0.13–0.7°, respectively.

reactions monitored in crystals. In the case of the intermolecular [2 + 2] and [4 + 4] photocycloadditions, the distance between directly reacting atoms decreased consistently as the photoreactions proceeded (Turowska-Tyrk, 2001, 2003; Turowska-Tyrk & Trzop, 2003). In the intramolecular processes the distance was constant from the beginning of the photoreactions to a certain degree of crystal conversion (Turowska-Tyrk, Bąkowicz & Scheffer; 2007; Turowska-Tyrk, Bąkowicz, Scheffer & Xia, 2006; Turowska-Tyrk, Trzop, Scheffer & Chen, 2006), and afterwards decreased markedly as in the Yang photocycloaddition of the salt of 1-(4-carboxybenzoyl)-1-methyladamantane with α-methylbenzylamine (Turowska-Tyrk, Trzop, Scheffer & Chen, 2006) and the retro-Claisen photorearrangement of the salt of 7-(4-carboxybenzoyl)norbornene with (*S*)-(−)-1-cyclohexylethylamine (Turowska-Tyrk, Bąkowicz, Scheffer & Xia, 2006). However, the distance probably declined from the beginning of the reaction in the case of the Yang photocycloaddition of the salt of 2-(4-carboxybenzoyl)-2-methyl-*endo*-bicyclo[2.1.1]hexyl with (*S*)-(−)-1-phenylethylamine (Turowska-Tyrk, Łabęcka, Scheffer & Xia, 2007).

Changes in the C9···C10^{i} distance are accompanied by changes in the C9—C16—C15^{i} and C10—C15—C16^{i} valence angles in reactant molecules (see Fig. 2 for atom labelling). As can be seen from Fig. 4, C9—C16—C15^{i} shows a distinct decrease after *ca* 40% crystal conversion. In turn, C10—C15—C16^{i} increases slightly until *ca* 20% photoproduct content, afterwards decreases significantly by 3.5 (6)°, and from *ca* 40% conversion stays statistically constant to the end of the photoreaction. The largest change of C9—C16—C15^{i} is 4.8 (8)°, from 112.41 (13) to 107.6 (8)°, and for C10—C15—C16^{i} is 3.8 (8)°, from 114.7 (4) to 110.9 (7)°. This shows certain elasticity of the ethylene bridges.

The C9—C10^{i} (and C10—C9^{i}) bond length in photoproduct molecules in the pure product crystal is 1.652 (3) Å, which is greater than for the normal single C—C bond (1.54 Å). The elongation of this bond in (2) was reported and discussed previously. The bond length determined for the first time by means of X-ray structure analysis was 1.77 Å (Ehrenberg, 1966), but this unusually high value was an artefact caused by coexistence in the crystal of the photoproduct and a certain amount of the reactant (Harada *et al.*, 1995, 1996). The distance was corrected to 1.66 Å (Harada *et al.*, 1995, 1996) and 1.648 (3) Å (Battersby *et al.*, 1995) on the basis of structure determination carried out for the pure photoproduct crystals. Neutron structure analysis gave the bond length as 1.64 (1) Å (Dougherty *et al.*, 1986). Similar long bonds were also observed for other ethylene-bridged bianthracenes (Toyoda *et al.*, 1985). High values were also found in theoretical calculations: 1.62–1.65 (Orimoto & Aoki, 2002), 1.64 (Zhou *et al.*, 1993), 1.64–1.67 (Battersby *et al.*, 1995) or 1.67–1.70 Å (Choi & Kertesz, 1997), depending on the basis sets.

The photoreaction of (1) causes a loss of aromatic character of the middle rings of the anthracene systems. The geometries of the middle rings before the photoreaction (*i.e.* in the pure reactant crystal) and after the photoreaction (*i.e.* in the pure product crystal) are compared in Table 3. It is easy to see

considerable lengthening of C10—C11, C10—C14, C9—C12 and C9—C13 due to a change of a bond order and smaller shortening of C11—C12 and C13—C14 (see Fig. 2 for atom labelling). Distinct changes are also observed for valence angles, the biggest changes are 10.3 (2) and 9.9 (2)° for C12—C9—C13 and C11—C10—C14, respectively.

3.4. Monitoring movements of the reactant and product molecule

It was observed for intra- and intermolecular photocycloadditions in crystals that molecules did not assume a fixed position during the photoreaction course (Fernandes & Levendis, 2004; Turowska-Tyrk, 2001, 2003; Turowska-Tyrk, Bąkowicz & Scheffer, 2007; Turowska-Tyrk, Bąkowicz, Scheffer & Xia, 2006; Turowska-Tyrk, Łabęcka, Scheffer & Xia, 2007; Turowska-Tyrk & Trzop, 2003; Turowska-Tyrk, Trzop, Scheffer & Chen, 2006). Reactant molecules moved smoothly from positions occupied in a pure reactant crystal owing to adaptation to the shape of the photoproduct, and product molecules moved towards positions occupied in a pure product crystal. The molecular movements possessed a rotational component. Fig. 5(*a*) presents variations in the angle between the anthracene system of reactant molecules and the *ab* plane for the photoreaction of (1). This angle changes only by 2.1 (6)°. For the *ac* and *bc* planes the variations are also smooth and small: 1.4 (6) and 1.4 (4)°. For photoproduct molecules the largest change for the analogous molecular plane is observed in the case of the *bc* plane: 3.4 (7)° (Fig. 5*b*). For the *ab* and *ac* planes the variations are smaller and not as smooth. This analysis indicates that both reactant and product molecules adopt more satisfactory positions in the crystal during the photoreaction. However, the observed angular changes are smaller than in the case of other intra- and intermolecular photoreactions. The largest change of molecular orientation reported so far was *ca* 22° (Turowska-Tyrk, Łabęcka, Scheffer & Xia, 2007). The much smaller changes observed for the photoreaction of (1) may result from larger similarities between the shapes, and also packing, of reactant and product molecules.

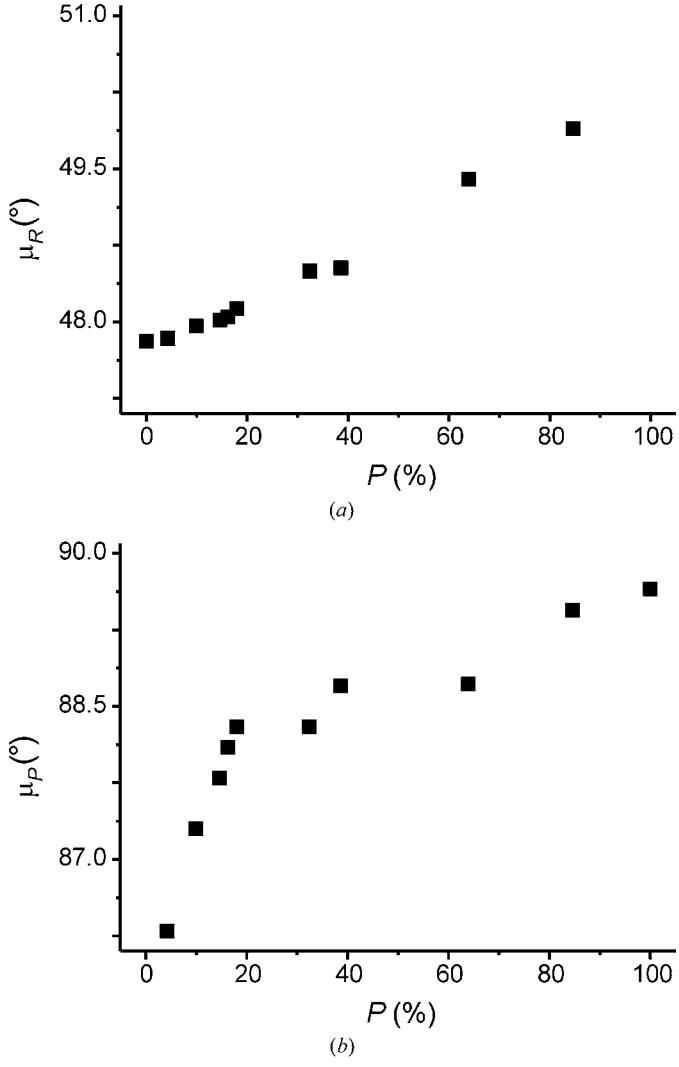

Figure 5
Variations in the angle between (*a*) the anthracene system of the reactant molecule and the *ab* plane, and (*b*) the analogous system of the photoproduct molecule and the *bc* plane. For better comparison the range of axes for both plots was set to be the same.

Table 3
Bond lengths and valence angles for the pure reactant and pure product crystals (Å, °).

	Reactant	Product
C9—C12	1.399 (2)	1.512 (3)
C9—C13	1.406 (2)	1.505 (3)
C10—C11	1.402 (2)	1.501 (3)
C10—C14	1.404 (2)	1.505 (3)
C11—C12	1.439 (2)	1.401 (3)
C13—C14	1.435 (2)	1.404 (4)
C9—C12—C11	119.53 (14)	115.9 (2)
C9—C13—C14	119.70 (15)	115.9 (2)
C10—C11—C12	119.61 (15)	116.7 (2)
C10—C14—C13	119.44 (14)	116.6 (2)
C11—C10—C14	118.10 (14)	108.19 (19)
C12—C9—C13	117.92 (14)	107.61 (19)
C13—C9—C16	121.60 (15)	118.0 (2)
C14—C10—C15	121.44 (15)	117.3 (2)

Table 4
Geometry of C—H$\cdots\pi$ hydrogen bonds and contacts in the pure reactant and pure product crystals (Å, °).

Crystal	$D\cdots A$	D—H	H$\cdots A$	D—H$\cdots A$
Pure reactant†	3.580	0.97	2.81	137.3
Pure product†	3.777	0.97	3.08	130.2

† Symmetry code for the acceptor: $x, \frac{3}{2}-y, -\frac{1}{2}+z$.

3.5. Hydrogen bonds

Molecules of (1) form weak C—H$\cdots\pi$ hydrogen bonds in the crystal. The C15 atom serves as a donor and the centre of the middle ring in the anthracene system of the neighbouring molecule serves as an acceptor of the H15*c* atom. Such bonds cannot exist among product molecules due to the loss of

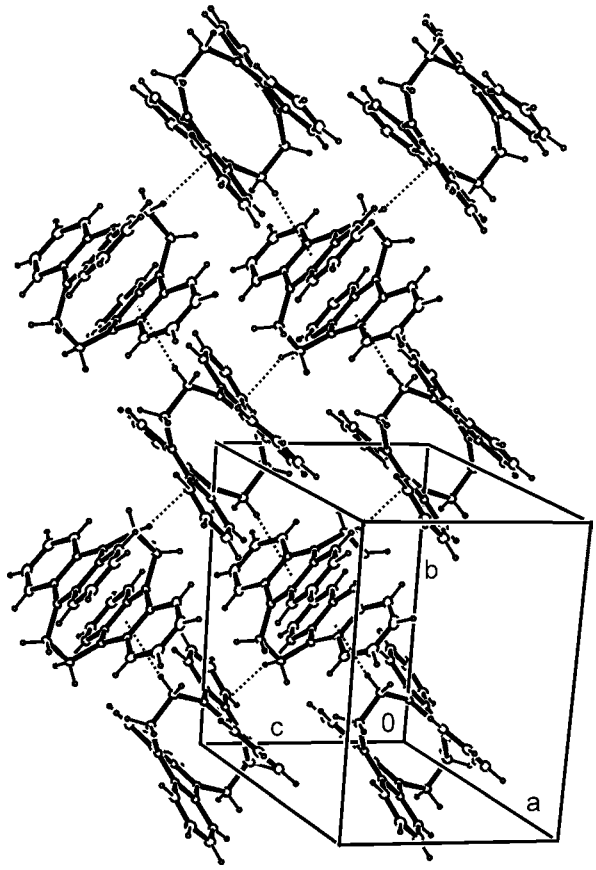

Figure 6
C—H$\cdots\pi$ hydrogen bonds in the pure reactant crystal.

aromatic character by the middle rings of the anthracene systems. However, the geometry of the contact between C—H and the centre of the middle ring is retained to a large extent. Table 4 presents the relevant data for the pure reactant and pure photoproduct crystals. The C—H$\cdots\pi$ bonds build a network nearly parallel to the *bc* plane (Fig. 6).

4. Conclusions

During single-crystal-to-single-crystal photochemical reactions only small shifts of atoms take place. In the presented studies, small displacements of atoms were monitored for the [4 + 4] photocycloaddition of (1). This provided detailed information about geometrical changes inside the crystal and molecules on the way leading from the pure reactant crystal to the pure product crystal. We described and explained the variations in:

(i) the cell constants and the cell volume,
(ii) the geometry of the reaction centre and
(iii) the orientation of reactant and product molecules.

The analysis of the shape and packing of reactant and product molecules enabled us to understand the changes of the cell constants and the orientation of molecules. Stress upon the reactant molecules resulting from the presence of product molecules and rigidity of reactant molecules were regarded as explaining the interesting variations in the reaction centre.

The authors thank Professor Jerzy Zoń and Tomasz Holband for the synthesis of bi(anthracene-9,10-dimethylene).

References

Battersby, T. R., Gantzel, P., Baldridge, K. K. & Siegel, J. S. (1995). *Tetrahedron Lett.* **36**, 845–848.
Choi, C. H. & Kertesz, M. (1997). *Chem. Commun.* pp. 2199–2200.
Dougherty, D. A., Choi, C. S., Kaupp, G., Buda, A. B., Rudziński, J. M. & Osawa, E. (1986). *J. Chem. Soc. Perkin Trans. II*, pp. 1063–1070.
Ehrenberg, M. (1966). *Acta Cryst.* **20**, 182–186.
Enkelman, V., Wegner, G., Novak, K. & Wagener, K. B. (1993). *J. Am. Chem. Soc.* **115**, 10390–10391.
Farrugia, L. J. (1997). *J. Appl. Cryst.* **30**, 565.
Fergusson, J. & Mau, A. W. H. (1974). *Mol. Phys.* **27**, 377–387.
Fergusson, J., Mau, A. W. H. & Morris, J. M. (1973). *Aust. J. Chem.* **26**, 91–102.
Fernandes, M. A. & Levendis, D. C. (2004). *Acta Cryst.* B**60**, 315–324.
Golden, J. H. (1961). *J. Chem. Soc.* pp. 3741–3748.
Harada, J., Ogawa, K. & Tomoda, S. (1995). *Chem. Lett.* pp. 751–752.
Harada, J., Ogawa, K. & Tomoda, S. (1996). *Mol. Cryst. Liq. Cryst.* **277**, 119–123.
Jones, W. & Theocharis, C. R. (1984). *J. Cryst. Spectrosc. Res.* **14**, 447–455.
Kaupp, G. (1972*a*). *Angew. Chem. Int. Ed.* **11**, 313–314.
Kaupp, G. (1972*b*). *Angew. Chem.* **84**, 259–261.
Kaupp, G. (1995). *Adv. Photochem.* **19**, 119–177.
Kaupp, G. (2002). *Curr. Opin. Solid State Mater. Sci.* **6**, 131–138.
Leibovitch, M., Olovsson, G., Scheffer, J. R. & Trotter, J. (1997). *J. Am. Soc. Chem.* **119**, 1462–1463.
Masnovi, J. M., Kochi, J. K., Hilinski, E. F. & Rentzepis, P. M. (1985). *J. Phys. Chem.* **89**, 5387–5395.
Milledge, J. (1962). *Proc. R. Soc. A*, **267**, 566–589.
Nakanishi, H., Jones, W., Thomas, J. M., Hursthouse, M. B. & Motevalli, J. M. (1980). *J. Chem. Soc. Chem. Commun.* pp. 611–612.
Nakanishi, H., Jones, W., Thomas, J. M., Hursthouse, M. B. & Motevalli, J. M. (1981). *J. Phys. Chem.* **85**, 3636–3642.
Novak, K., Enkelmann, V., Wegner, G. & Wagener, K. B. (1993*a*). *Angew. Chem. Int. Ed. Engl.* **32**, 1614–1616.
Novak, K., Enkelmann, V., Wegner, G. & Wagener, K. B. (1993*b*). *Angew. Chem.* **105**, 1678–1680.
Ohba, S. & Ito, Y. (2003). *Acta Cryst.* B**59**, 149–155.
Orimoto, Y. & Aoki, Y. (2002). *Int. J. Quantum Chem.* **86**, 456–467.
Oxford Diffraction Ltd (2003). *Xcalibur CCD CrysAlis*, Version 1.170. Oxford Diffraction Ltd, Wrocław, Poland.
Scheidt, W. R. & Turowska-Tyrk, I. (1994). *Inorg. Chem.* **33**, 1314–1318.
Sheldrick, G. M. (2008). *Acta Cryst.* A**64**, 112–122.
Theocharis, C. R., Nakanishi, H. & Jones, W. (1981). *Acta Cryst.* B**37**, 756–758.
Toyoda, T., Kasai, N. & Misumi, S. (1985). *Bull. Chem. Soc. Jpn*, **58**, 2348–2356.
Turowska-Tyrk, I. (2001). *Chem. Eur. J.* **7**, 3401–3405.
Turowska-Tyrk, I. (2003). *Acta Cryst.* B**59**, 670–675.
Turowska-Tyrk, I., Bąkowicz, J. & Scheffer, J. R. (2007). *Acta Cryst.* B**63**, 933–940.
Turowska-Tyrk, I., Bąkowicz, J., Scheffer, J. R. & Xia, W. (2006). *CrystEngComm*, **8**, 616–621.
Turowska-Tyrk, I. & Trzop, E. (2003). *Acta Cryst.* B**59**, 779–786.
Turowska-Tyrk, I., Trzop, E., Scheffer, J. R. & Chen, S. (2006). *Acta Cryst.* B**62**, 128–134.
Turowska-Tyrk, I., Łabęcka, I., Scheffer, J. R. & Xia, W. (2007). *Pol. J. Chem.* **81**, 813–824.
Wada, A. & Tanaka, J. (1977). *Acta Cryst.* B**33**, 355–360.
Zhou, X., Liu, R. & Allinger, N. (1993). *J. Am. Chem. Soc.* **115**, 7525–7526.